JOURNAL OF PROPULSION AND POWER
Vol. 27, No. 1, January–February 2011

Vane Clocking Effects on the Resonant Response of an Embedded Rotor

Yoon S. Choi,* Nicole Key,* and Sanford Fleeter†
Purdue University, West Lafayette, Indiana 47907

DOI: 10.2514/1.48485

This paper addresses the effect of vane clocking and steady loading on the resonant response of an embedded rotor. The technical approach is centered on experimentally quantifying the effect of vane clocking on the resonant response of integrally bladed rotors in the Purdue University three-stage highly loaded compressor, a geometry representative of the rear stages of a high pressure compressor with similar vane counts. The first torsion mode resonant response of integrally bladed rotor 2 generated by the wakes from the upstream stators is quantified nonintrusively using an Agilis nonintrusive stress measurement system for six vane clocking configurations at the design and high loading conditions. The forcing function to integrally bladed rotor 2 consists of the stator 1 wakes and the potential fields from stators 1 and stator 2, and their aerodynamic interactions. Thus, the integrally bladed rotor 2 resonant response experiments involve classic vane clocking, with the inlet guide vane, stator 1 and stator 2 each having identical vane counts. The data show high responding individual blades on the rotor, i.e., the effect of mistuning on resonant response, and demonstrate the viability of vane clocking for passive control of resonant response including resulting in configurations with no high responding individual blades.

I. Introduction

EACH new generation of gas turbine engine is required to have increased thrust-to-weight ratio, with the design approach to achieving this involving increase flow through the engine and fewer parts. This is accomplished with new compressor designs with higher tip speeds, lower aspect ratio blading, more closely spaced blade rows and fewer stages. As a result, advanced compressors use thin low aspect ratio airfoils which when combined with the increased flow through the engine, result in a significant increase in the aerodynamic loading and corresponding high steady-state stresses. Also, the mechanical damping is considerably reduced in newer rotor designs, particularly those with integrally bladed rotor (IBR) configurations and in those without shrouds. As a result, high cycle fatigue (HCF) and resonant response of turbomachine blading resulting from flow-induced vibrations continues to be a significant problem throughout the gas turbine industry. Design resonant response analyses consider a tuned blade row, i.e., a rotor with all blades having the same structural properties and thus, identical natural frequencies. In fact, there are small blade-to-blade variations, termed mistuning, which are known to lead to significant variations with both increased and decreased blade resonant response amplitudes as compared with that of the tuned blade row, with mistuning cited as an HCF source.

Turbomachinery rotors have typically been bladed-disks, with individual blades inserted into a slotted disk and retained by means of a dove-tail or fir-tree attachment. Advances in manufacturing techniques have resulted in bladed-disks with increased uniformity, i.e., small mistuning. Unfortunately, smaller mistuning does not translate into lower amplitude blade vibrations. In addition, to improve rotor aerodynamic performance, new manufacturing techniques have enabled IBRs wherein the blades and disk are machined from a single piece of material, to be used. IBRs thus eliminate the need to attach the blades to the disk, thereby decreasing the number of parts, and decrease the drag and increase the compressor efficiency. As compared with bladed-disks, IBRs have both much smaller mistuning and mechanical damping. IBRs thus exacerbate the potential for large amplitude resonant response and HCF because of reduced mechanical damping and mistuning.

The implementation of IBRs into engine designs also affects the development of acceptable rotors. When bladed-disks are found to have unacceptably high vibration amplitudes and vibratory stress during development or in the field, a traditional approach is to incorporate friction dampers. However, resonant response problems in IBRs may not be able to be solved with friction dampers because they cannot be easily implemented. Hence, new solutions are required to address IBR resonant response problems.

In this regard, vane clocking is a potential technique for the control of the resonant response of embedded rotors. A particular embedded rotor is subjected to the periodic passing of the wakes from the upstream airfoil row and the potential disturbances from both the upstream and the downstream airfoils rows, i.e., an embedded rotor is subjected to three forcing functions, Fig. 1. With airfoil rows having similar vane counts, the stationary vane rows can be indexed relative to one another to affect the airfoil row unsteady aerodynamic interactions. This circumferential indexing of vanes in adjacent rows with similar vane counts is termed vane clocking. Experimental research has shown that vane clocking can be an effective tool to increase turbine performance [1–4], increase compressor performance [5], enhance turbine heat transfer [6], and decrease the unsteady aerodynamic forces on the blades, thereby affecting discrete frequency noise generation [7–9].

In a three-stage low-speed compressor, Capece and Fleeter [10] showed that while indexing the upstream stator had no effect on the steady loading of the downstream vane row, vane indexing did have a large impact on the unsteady aerodynamic forcing function. Sanders and Fleeter [11] developed a linear theory model to investigate vane clocking as a means of passive control of blade unsteady loading, predicting significant reductions in unsteady lift and moment. Hsu and Wo [12] measured a 60% reduction of the stator force amplitude in a rotor-stator rotor large-scale, low-speed axial compressor by clocking the downstream rotor. Mailach and Vogeler [13] performed experiments in a low-speed compressor, with blade surface unsteady pressures measured at midspan on a single stage-three blade. There were significant changes in the unsteady pressure distribution on rotor 3 even with the vane indexing of stator 1 and stator 4. A

Presented as Paper 2008-4793 at the 44th AIAA/ASME/SAE/ASEE Joint Propulsion Conference and Exhibit, Hartford, CT, 21–23 July 2008; received 9 December 2009; revision received 24 May 2010; accepted for publication 17 September 2010.

*Graduate Research Assistant, Mechanical Engineering, 500 Allison Road. Student Member AIAA.

†McAllister Distinguished Professor, Mechanical Engineering, 500 Allison Road. Fellow AIAA.

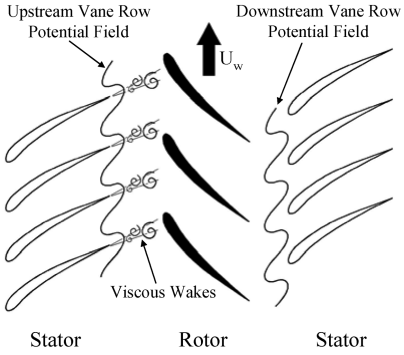

Fig. 1 Unsteady aerodynamic forcing functions to an embedded rotor.

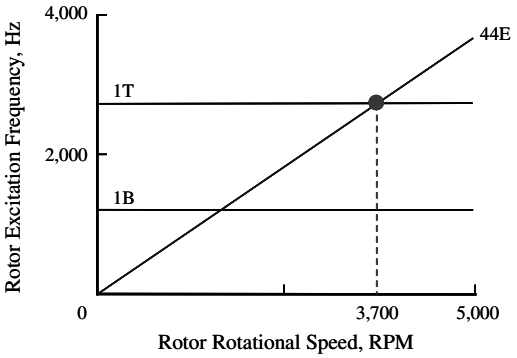

Fig. 3 IBR 2 Campbell diagram for modes with 11*ND*.

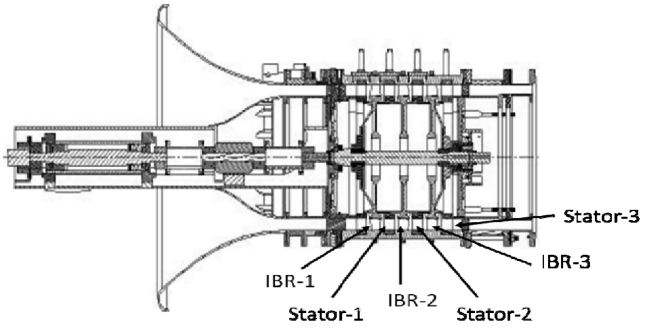

Fig. 2 Purdue three-stage compressor.

computational study by Li and He [14] supported the experimental work on a 1.5 stage transonic turbine by Miller et al. [15]. Parametric studies with various stator blade counts showed that circumferential variation of the unsteady forcing is a function of the NGV-stator blade count difference, but the local stator forcing magnitude is affected by its clocking position. However, none of these studies addressed the effect of vane clocking on rotor resonant response.

This paper addresses the effect of vane clocking and steady loading on the resonant response of an embedded rotor. The technical approach is centered on experimentally quantifying the effect of vane clocking on the resonant response of IBRs in the Purdue University three-stage highly loaded compressor, a geometry representative of the rear stages of a high pressure compressor with similar vane counts. This compressor has an inlet guide vane (IGV) followed by three stages each composed of an IBR and a vane row, with all vane rows individually indexable, enabling the vanes to be clocked. The effect of steady loading on the first torsion mode resonant response of the second stage rotor, IBR 2, generated by the wakes from the upstream stators is quantified nonintrusively using a state-of-the-art Agilis nonintrusive stress measurement system (NSMS) for six vane clocking configurations at the design and high loading conditions. The forcing function to IBR 2 consists of the first stage vane (stator 1) wakes and the potential fields from the first stage vanes (stators 1) and the second stage vanes (stator 2), and their aerodynamic interactions (Fig. 2).

II. Experimental Approach

The Purdue three-stage compressor is axial-flow geometry aerodynamically representative of the aft stages of a Rolls-Royce Corporation high-pressure compressor, with the three IBRs, IBR 1, IBR 2 and IBR 3 (Fig. 2). This compressor has mean diffusion factors in the range of $0.433 \sim 0.464$. The design overall pressure ratio is 1.31.

The hub and tip diameters are 20 and 24 in., respectively. The IGV profiles are double circular arcs (DCAs) with 44 vanes, and the rotor blades are also DCA profiles with 36 blades for IBR 1, 33 blades for IBR 2, and 30 blades for IBR 3. The remaining vanes are NACA 65 Series airfoils with 44 vanes for stator 1 and stator 2 and 50 vanes for stator 3. The design speed is 5000 rpm.

A finite element analysis was performed to predict the IBR 2 and IBR 3 natural frequencies, the corresponding mode shapes, and to identify the critical resonant conditions [16]. The resulting Campbell diagram for IBR 2 is presented in Fig. 3. The resonant responses of the 33 blades of IBR 2 are excited by the 44 upstream and downstream stator vanes. The 44 upstream stator vanes excite the rotor at 44 times the engine speed, with this excitation frequency indicated by the 44E line. This 44E line crosses the first torsion mode at approximately 3700 rpm, with this resonant crossing closest to the design speed of 5000 rpm.

III. NSMS Data Acquisition System

The IBR 2 response measurements are performed nonintrusively, accomplished using an Agilis NSMS tip-timing system. Optical blade-tip sensors mounted in the casing along the blade-tip circumferential path provide measurements quantify the time of arrival of each blade, hence the term tip-timing. The functional components of NSMS include blade-tip and shaft-revolution optical probes, signal conditioners, signal processing circuitry, and a processor with high-speed counter/timer cards. A laser beam is passed through fiber optics to the casing mounted optical probes. When a blade tip passes beneath a probe, light is reflected back and transmitted to a photo detector whose signal is sent to a pulse-to-digital converter. The converter uses a digital clock to time the blade passing events relative to the 1/rev shaft-revolution optical probe pulse.

The NSMS optical sensors are positioned to model the blade tip vibration, reduce the noise level, and obtain valid data fits. The optimum circumferential probe locations are determined from the expected resonant responses in the operating range via software. Agilis software generates an optimization function from a combination of response models which consist of single, double, triple, or quad combinations of expected engine order. For a given probe set, each model has a unique condition number, with a unity value for the optimum probe set. The condition numbers for each model are recombined with a target weighting into a global optimization function. The optimization is run using a simulated annealing algorithm until the best probe locations are obtained within the specified number of iterations.

To measure the blade tip deflection, the Agilis NSMS data acquisition system uses eight fiber optic spot probes to both send light and detect reflected light. The laser module generates laser light and is controlled through an Ethernet cable from a personal

Table 1 NSMS resolution

Rpm	Resolution, mils
2000	0.005
3000	0.008
3700	0.009
4000	0.010
5000	0.013

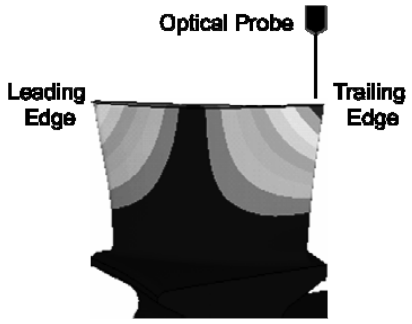

Fig. 4 Three-stage IBR predicted first torsion mode [17].

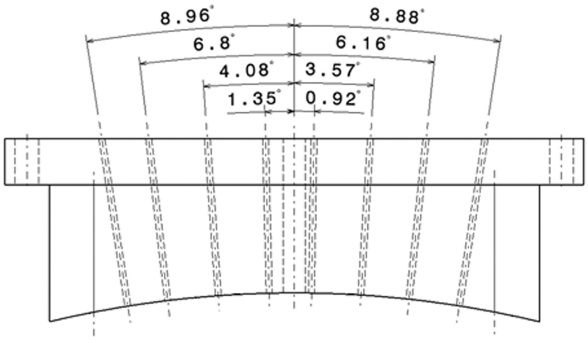

Fig. 5 Optimum 8 NSMS probe locations.

computer. It provides light through a supply fiber optic to a case-mounted optical probe. As the blade tip passes the case-mounted probe, the laser light is reflected and transmitted through return fiber optics to the detector module, with the output signals transmitted to the PC.

The resolution of the NSMS measurements is determined by the clock speed of the counter timer board, the rotor tip diameter, and the rotor tip speed [Eq. (1)]:

$$\text{Resolution} = \frac{\pi d}{T_{\text{speed}}} \tag{1}$$

where d is the rotor tip diameter and T_{speed} is the rotor tip speed.

The Agilis NSMS sampling period is $\tau_{\text{sp}} = 1/500,000$ sec / sample and the tip diameter is 24 in. for IBR 2. The theoretical resolution of the NSMS data is summarized in Table 1. At the resonance condition of interest, the ideal resolution of the NSMS data is 0.009 mils at 3700 rpm.

The NSMS optical probes are positioned on the case window so as to detect the blade first torsion mode vibration, with a signal-to-noise ratio which enables the data to be analyzed. Based on the non-dimensional first torsion mode shape, the case-mounted optical probes are positioned 0.05 in. forward of the IBR 2 blade trailing edges where the maximum tip deflection is predicted, Fig. 4.

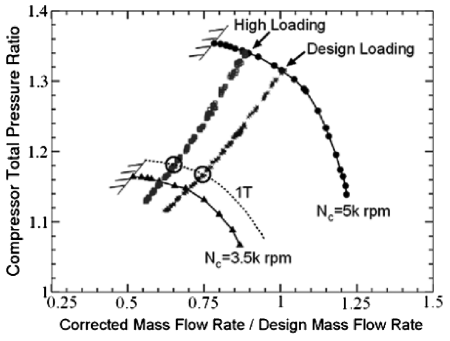

Fig. 6 Three-stage compressor performance.

The Agilis arrival time analysis probe location optimization software is used to determine the circumferential locations of eight optical NSMS probes for IBR 2. For these experiments, the analysis considered the 8 probes to be circumferentially distributed in a $\pm 20°$ window sector with a minimum probe spacing of 2°. The resulting condition number is 1.06, with a unity value for the optimum probe set. with the optimized circumferential probe locations shown in Fig. 5.

IV. Experiments

A. Compressor Performance

The effect of steady loading on the first torsion mode resonant response of IBR 2 is investigated at the design and high loading operating conditions, indicated on the performance map presented in Fig. 6. The compressor is brought to a steady operating condition at the design speed of 5000 rpm. The NSMS data are then acquired during a constant transient through the resonance at approximately 3700 rpm at a sweep rate of 4.5 rpm/s, a value lower than the critical sweep rate of 5 rpm/s. Note that the critical sweep rate is defined as the ratio of the half-power bandwidth taken over three stress cycles, i.e., three cycles must be completed within the half-power bandwidth around the resonance. The NSMS data are acquired during six transients composed of three consecutive accelerations and decelerations. The maximum first torsion blade response amplitude data are analyzed and normalized by the mean response amplitude.

B. Wake Forcing Functions to IBR 2

Six vane clocking configurations are used for these resonant response experiments, Fig. 7. The clocking configuration is defined by the stator 1% vane passage location minus the stator 2% vp location. The six configurations are 0, 15, 32, 49, 66, and 83% vp and are referred to as CL-1, CL-2, CL-3, CL-4, CL-5, and CL-6, respectively. A clocking offset of 100% vp would be the same relative vane position for 0% vp.

The forcing function to IBR 2 consists of the stator 1 wakes, the potential fields from stators 1 and stator 2, and their aerodynamic interactions. At 3500 rpm close to the resonant speed of interest, the wake forcing functions from stator 1 at design and high loading were measured using a Kiel head total pressure probe. Figure 8 shows the stator 1 wake profile at 88% span for the design and high loading conditions, with six vane clocking positions. As expected, the stator 1 wakes at high loading are apparently deeper and wider than those at design loading, but there is a very small variation in wake profile associated with vane clocking. Thus, any variation in the measured resonance response of the embedded rotor is attributed to differences in the wake forcing function since these are differences are negligible although there may be wake variations at the tip which are not measured.

C. NSMS Data

The variations from the first torsion mean frequency are measured with the NSMS, with the measured stiffness of each blade presented in terms of its frequency deviation from the rotor mean $\delta\omega_j/\bar{\omega}$ at an operating condition. The frequency distribution of IBR 2 at the CL-1 vane position at the design loading is shown in Fig. 9.

At each loading condition, NSMS data were acquired during three accelerations and three decelerations through the resonance. These

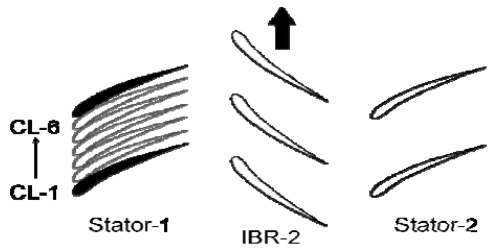

Fig. 7 Vane clocking configurations.

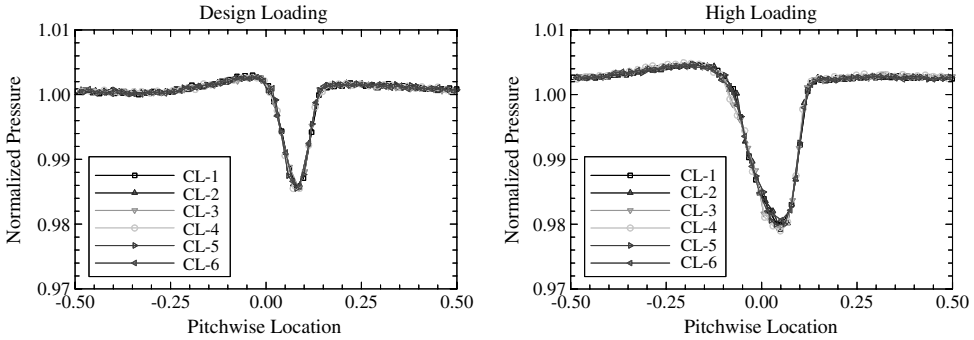

Fig. 8 Stator-1 wake forcing functions to IBR 2 at 3500 rpm.

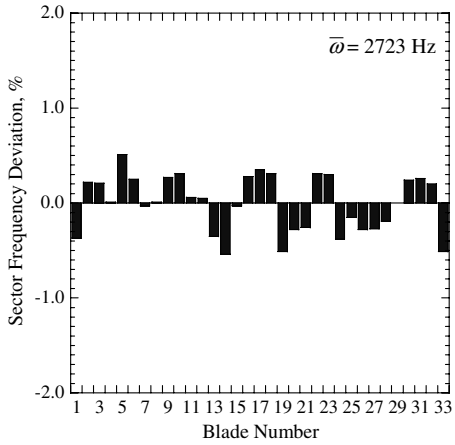

Fig. 9 First torsion frequency mistuning at design loading.

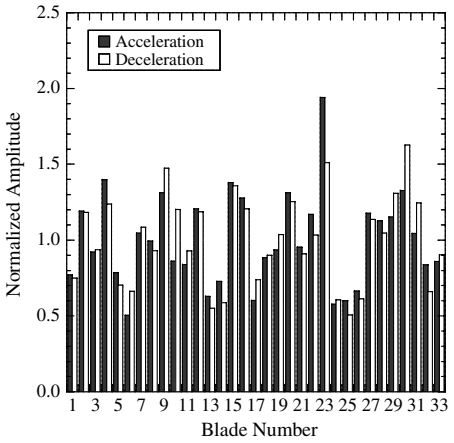

Fig. 11 IBR 2 first torsion blade-to-blade normalized response for the largest difference data set between acceleration and deceleration: CL-6 at design loading.

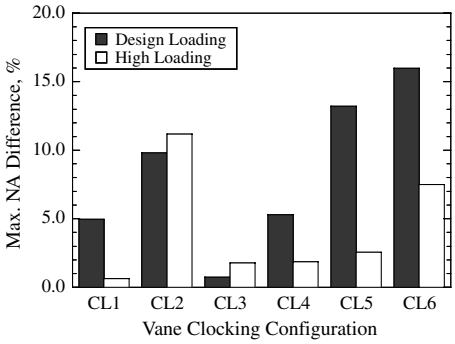

Fig. 10 IBR 2 first torsion maximum normalized blade response differences between acceleration and deceleration at vane clocking configurations.

data are analyzed and the response amplitude of each blade tip determined as well as the mean response amplitude of all of the blades. Vane clocking position CL-1 with all vanes aligned is the nominal clocking position. At CL-1, the mean blade response of all blades is 8.21 mils at design and by 14.62 mils at high loading. At the other vane clocking positions, the individual blade-to-blade responses are normalized by these mean amplitudes at CL-1, i.e., the blade responses are normalized by 8.21 mils at design and by 14.62 mils at high loading with the result termed the normalized amplitude.

At each loading condition, NSMS data were acquired during three accelerations and three decelerations through the resonance. The largest differences in the normalized maximum response data for the three accelerations and decelerations of each IBR at design and high loading are presented in Fig. 10. The CL-3 vane clocking position has normalized amplitude differences less than 2% at all loadings. The largest normalized amplitude difference for CL-6 vane position is 16% at design loading.

These differences in the normalized maximum response data for the three accelerations and decelerations have only a minimal effect on the blade-to-blade normalized response. This is demonstrated in Fig. 11 which presents the blade-to-blade normalized response for the largest difference data sets for the CL-6 vane position at the design loading condition. Between acceleration and deceleration, Blade 23 or 30 is the highest or high responder, and overall blades have very similar high and low responders.

V. Results: IBR 2 Resonant Response

The effects of vane clocking on the first torsion mode resonant response of IBR 2 is experimentally investigated at the design and high loading operating points. Data analyzed show the effect of vane clocking and steady loading on the blade-to-blade normalized response and the maximum normalized response, i.e., with the blade response normalized by the mean amplitudes at CL-1 for each steady loading, as well as the mean blade response.

A. Blade-to-Blade Response

The effect of vane clocking on the rotor blade-to-blade response distributions at both the design and high steady loading operating points is presented in Fig. 12. At both steady loading conditions, the blade-to-blade response distributions are similar at each vane clocking configuration, exhibiting a periodic variation around the rotor with relatively low normalized response amplitude in the vicinity of Blades 6, 13, 25 for example. Also, there are individual high responding blades at all clocking configurations at both loading levels, with the exception of CL-3 at high loading. Note that individual high responding blades would experience vibratory stress levels much greater than the mean and, thus, would be the blades that result in HCF. Thus, CL-3 at high loading with no high responding individual blades would not experience HCF resulting from mistuning.

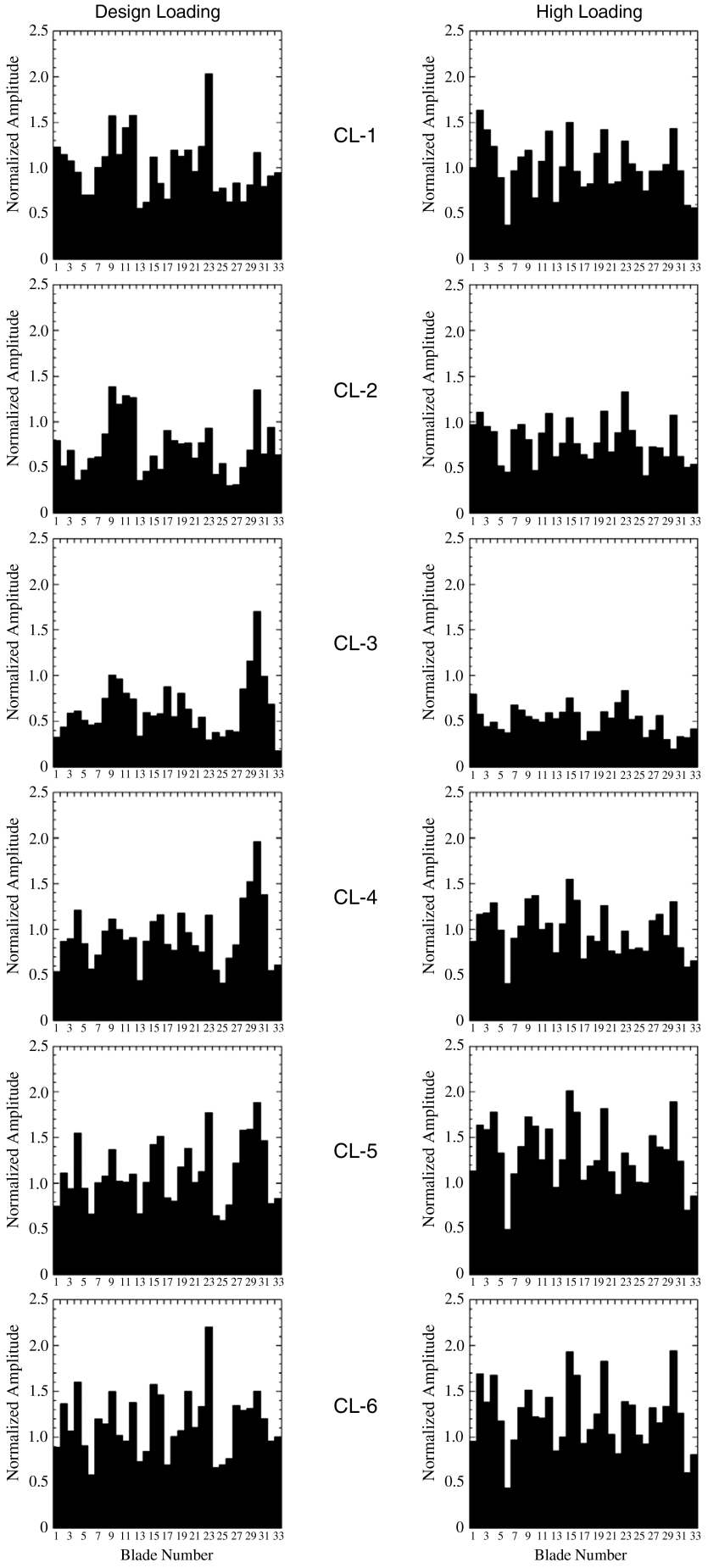

Fig. 12 Vane clocking effect on normalized blade response at design and high loading.

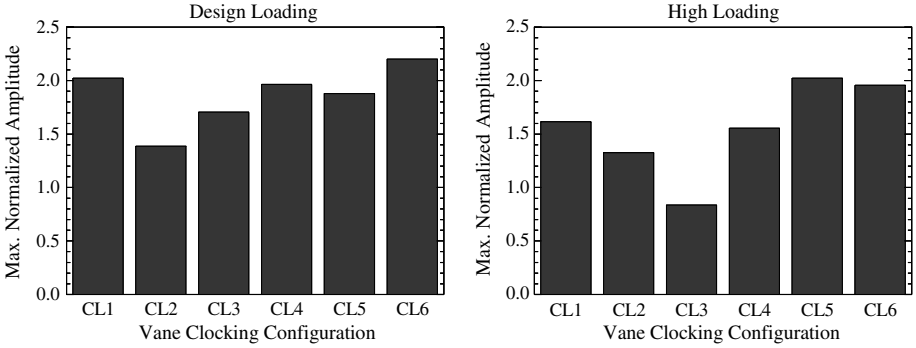

Fig. 13 IBR 2 first torsion maximum normalized blade response.

At both the design and high steady loading operating points, CL-5 and CL-6 result in the largest number of high responding individual blades, i.e., blades having normalized amplitudes equal to or greater than 1.5, with CL-2 at both steady loadings having no blades with normalized amplitudes greater than 1.5 but still with high responding individual blades. ForCL-3 at high loading, there are no blades with normalized amplitudes greater than 1.5 and no high responding indivdial blades, with all blades with normalized amplitudes less than one. These data thus demonstrate that at high loading there is a vane clocking configuration that results in minimum resonant response with no high responding individual blades.

At the design loading, Blades 9 and 30 are relatively high responders at all clocking configurations. Blade 30 is the highest responder for CL-3, CL-4, and CL-5, with normalized amplitudes of 1.71, 1.96 and 1.88, respectively. Blade 9 with normalized amplitude of 1.39 is the highest responder for clocking configuration 2. Blade 23 is the highest responder for CL-1 and CL-6, with normalized amplitudes of 2.02 and 2.20, respectively.

Steady loading affects which blades are the high responding blades as well as the maximum blade response amplitude. For example, Blade 15 is always a high responder at the high loading but not at the design loading. For CL-1, Blade 23 is the high responding blade at the design loading and a high responder at high loading. However, Blade 2 is the highest responder at high loading but a moderate responder at the design loading. For CL-2, Blade 23 is the highest responding blade at high loading but a moderate responding blade at design loading. Blade 9 is the highest responder at design loading, but a moderate responder at high loading. Blade 10 is the high responder at the design loading, but is a low responder at high loadings. At CL-3, Blade 30 is the highest responding blade at design loading but the lowest responder at high loading. Blade 23 is a low responder at design loading but the highest responding blade at high loading. Blade 1 is a high responding blade at high loading, but is only a low responder at design loading. For CL-4, Blade 30 is the highest responding blade at design loading, and is also a high responder at high loading. Blade 15 is the highest responding blade at the high loading, and a relatively moderate responder at design loading. Blades 6, 13, and 25 are the low responders at both design and high loadings. For CL-5 , Blade 30 is the highest responding blade at design loading, and is also a high responder at high loading.

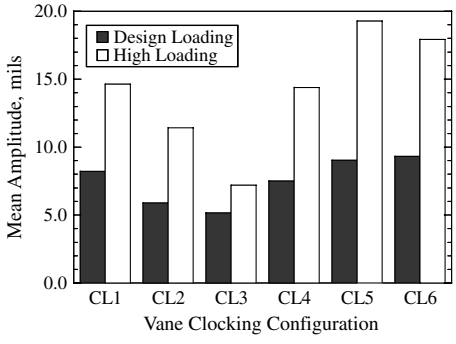

Fig. 14 IBR 2 first torsion mean blade response.

Blade 15 is the highest responding blade at the high loading, and a relatively moderate responder at design loading. Blades 6 and 32 are the low responders at both design and high loadings. At CL-6, Blade 23 is the highest responding blade at design loading, but is a moderate responder at high loading. Blade 30 is the highest responding blade at the high loading, but a relatively moderate responder at design loading.

B. Maximum Normalized Blade Response

Figure 13 shows the effect of vane clocking on the blade maximum normalized response amplitude. At both loading levels, there is a clocking position that results in a minimum: maximum normalized amplitude of 1.39 for CL-2 at design loading and 0.83 for CL-3 at high loading. At the design loading, only CL-2 has a maximum normalized amplitude less than 1.5, with CL-1, CL-3, CL-4, CL-5 and CL-6 all having maximum normalized amplitudes greater than 1.5, and CL-1 and CL-6 greater than 2. At the high loading condition, CL-1, CL-4, CL-5 and CL-6 all have maximum normalized amplitudes greater than 1.5, with CL-5 having a maximum normalized amplitude greater than 2 and CL-6 nearly 2 (1.96). The maximum difference of maximum normalized amplitudes for six vane clocking positions is 58% at design loading and 143% at high loading.

C. Mean Blade Response

The IBR 2 blade mean response amplitude variation with vane clocking at both the design and high loading conditions is shown in Fig. 14. Clocking configuration CL-3 shows the minimum mean vane response at both design loading and high loading: 5.16 mils and 7.20 mils. The maximum mean vane response occurs for CL-6 at design loading and CL-5 at high loading: 9.31 mils and 19.28 mils. There is a large increase in the rotor mean response with increased loading. The amplitude of the maximum mean vibration at high loading is more than double that at design loading, but the clocking configurations that give the minimum and maximum mean response do not vary significantly between loading conditions. The only change occurs in the maximum mean response which goes from CL-6 at design loading to CL-5 at high loading. However, it should be noted that the difference between the mean amplitude for CL-5 and CL-6 at high loading is quite small. The maximum difference of mean amplitudes for six vane clocking positions is 80% at design loading and 168% at high loading.

VI. Conclusions

The experimental investigation of vane clocking for control of resonant response was performed in the Purdue three-stage compressor which has geometry representative of the rear stages of a high pressure compressor. This compressor has an IGV row followed by three stages, with all vane rows indexable, enabling the vanes to be clocked. A nonintrusive tip-timing system was used to measure the first torsion mode resonant response of IBR 2 with the upstream and downstream vane rows clocked to six configurations. Thus, the variation in the IBR 2 resonant response caused by altering the forcing function to these rotors by vane clocking was investigated.

The forcing function to IBR 2 consists of the stator 1 wakes and the potential fields from stators 1 and stator 2, and their aerodynamic interactions.

The NSMS data revealed that the blade-to-blade response distributions were similar at each vane clocking configuration, exhibiting a periodic variation around the rotor. Also, there were high responding individual blades at all clocking configurations at both loading levels, with the exception of CL-3 at high loading. As individual high responding blades would experience vibratory stress levels much greater than the mean and, thus, would be the blades that result in HCF, CL-3 at high loading with no high responding individual blades would not experience HCF resulting from mistuning.

At both loading levels, there was a clocking position that results in a minimum resonant response. Clocking configuration CL-3 resulted in the minimum mean vane response at both design loading and high loading, with the maximum mean vane response found for CL-6 at design loading and CL-5 at high loading. Also, there was is a large increase in the rotor mean response with increased loading. For the high responding blades, there was a minimum in the maximum normalized amplitude of 1.39 for CL-2 at design loading and 0.83 for CL-3 at high loading.

To gain insight into the flow physics associated with vane clocking, AU3D, an implicit, unsteady, unstructured, compressible flow solver was used to compute the vane clocking effects on the resonant response of rotor 2, with these predictions correlated with the data presented herein [17]. The predictions were predicted the clocking configurations for the two lowest responses, CL-2 and CL-3, and the two highest responses, CL-5 and CL-6. The pressure field predictions revealed that the configuration with the lowest response (CL-2) placed the S1 wakes on the S2 leading edge. The configuration with the highest response (CL-5) placed the S1 wakes in the midpassage of the S2 vane row.

These experiments have thus demonstrated the viability of vane clocking for passive control of resonant response including reducing the blade mean resonant response and resulting in configurations with no high responding individual blades, thereby minimizing or eliminating the detrimental effects of mistuning.

Acknowledgment

The authors wish to thank Roy Fulayter of Rolls-Royce for his insight and guidance on this project.

References

[1] Huber, F. W., Johnson, P. D., Sharma, O. P., Staubach, J. B., and Gaddis, S. W., "Performance Improvement Through Indexing of Turbine Airfoils: Part 1: Experimental Investigation," *Journal of Turbomachinery*, Vol. 118, No. 4, 1996, pp. 630–635. doi:10.1115/1.2840918

[2] Reinmöller, U., Stepha, B., Schmit, S., and Niehuis, R., "Clocking Effects in a 1.5 Stage Axial Turbine: Steady and Unsteady Experimental Investigation Supported by Numerical Simulations," *Journal of Turbomachinery*, Vol. 124, No. 1, 2002, pp. 52–60. doi:10.1115/1.1425811

[3] Haldeman, C. W., Dunn, M., Barter, J. W., Green, B. R., and Bergholz, R. F., "Experimental Investigation of Vane Clocking in a One and One-Half Stage High Pressure Turbine," *Journal of Turbomachinery*, Vol. 127, No. 3, 2005, pp. 512–521. doi:10.1115/1.1861915

[4] Behr, T., Porreca, L., Mokulys, T., Kalfas, A. I., and Abhari, R. S., "Multistage Aspects and Unsteady Effects of Stator and Rotor Clocking in an Axial Turbine with Low Aspect Ratio Blading," *Journal of Turbomachinery*, Vol. 128, No. 1, 2006, pp. 11–22. doi:10.1115/1.2101855

[5] Key, N., Lawless, P., and Fleeter, S., "An Experimental Study of Vane Clocking Effects on Embedded Compressor Stage Performance," American Society of Mechanical Engineers Paper GT2008-51087, American Society of Mechanical Engineers Turbo Expo, Berlin, 9–13 June 2008.

[6] Johnston, D. A., and Fleeter, S., "Turbine Blade Unsteady Heat Transfer Change due to Stator Indexing," American Society of Mechanical Engineers Paper 1999-GT-0376, 1999.

[7] Walker, G. J., and Oliver, A. R., "The Effect of Interaction Between Wakes from Blade Rows in an Axial Flow Compressor on the Noise Generated by Blade Interaction," *Journal of Engineering for Power*, Vol. 94, No. 4, 1972, pp. 241–248. doi:10.1115/1.3445679

[8] Schmidt, D. P., and Okiishi, T. H., "Multistage Axial-Flow Turbomachine Wake Production, Transport, and Interaction," *AIAA Journal*, Vol. 15, No. 8, 1977, pp. 1138–1145. doi:10.2514/3.60765

[9] Kamiyoshi, S., and Kaji, S., "Tone Noise Reduction of Multi-Stage Fan by Airfoil Clocking," AIAA Paper 2000-1992, June 2000.

[10] Capece, V. R., and Fleeter, S., "Unsteady Aerodynamic Interactions in a Multistage Compressor," *Journal of Turbomachinery*, Vol. 109, No. 3, 1987, pp. 420–428. doi:10.1115/1.3262122

[11] Sanders, A. J., and Fleeter, S., "Vane Row Indexing for Passive Vibration Control of Axial Flow Turbomachine Rotors," AIAA Paper 1995-2656, 1995.

[12] Hsu, S. T., and Wo, A. M., "Reduction of Unsteady Blade Loading by Beneficial Use of Vortical and Potential Disturbances in an Axial Compressor with Rotor Clocking," *Journal of Turbomachinery*, Vol. 120, No. 4, 1998, pp. 705–713. doi:10.1115/1.2841781

[13] Mailach, R., and Vogeler, K., "Rotor-Stator Interaction in a Four-Stage Low-Speed Axial Compressor. Part 1: Unsteady Profile Pressure and the Effect of Clocking," *Journal of Turbomachinery*, Vol. 126, No. 4, 2004, pp. 507–518. doi:10.1115/1.1791641

[14] Li, H. D., and He, L., "Blade Count and Clocking Effects on Blade Row Interaction in a Transonic Turbine," *Journal of Turbomachinery*, Vol. 125, No. 4, 2003, pp. 632–640. doi:10.1115/1.1622711

[15] Miller, R. J., Moss, R. W., Ainsworth, R. W., and Harvey, N. W., "Wake, Shock, and Potential Field Interactions in a 1.5 Stage Turbine. Part 2: Vane–Vane Interaction and Discussion of Results," *Journal of Turbomachinery*, Vol. 125, No. 1, 2003, pp. 40–47. doi:10.1115/1.1508387

[16] Fulayter, R. D., "An Experimental Investigation of Resonant Response of Mistuned Fan and Compressor Rotors Utilizing NSMS," Ph.D. Dissertation, Purdue Univ., School of Mechanical Engineering, West Lafayette, IN, May 2004.

[17] Salontay, J. R., Key, N. L., and Fulayter, R. D., "A Computational Investigation of Vane Clocking Effects on Compressor Forced Response," AIAA Paper 2010-746, July 2010.

R. Miller
Associate Editor